

1 Long-term ensemble forecast of snowmelt inflow into the 2 Cheboksary reservoir under the two different weather scenarios

3 Alexander Gelfan^{1,2}, Vsevolod Moreydo¹, Yury Motovilov¹, Dimitri Solomatine^{1,3,4}

4 ¹Water Problems Institute of Russian Academy of Sciences, Watershed Hydrology Lab., Moscow, Russia

5 ²Moscow State University, Geographical Department, Moscow, Russia

6 ³IHE Delft Institute for Water Education, Chair of Hydroinformatics, Delft, the Netherlands

7 ⁴Delft University of Technology, Water Resources Section, Delft, the Netherlands

8 *Correspondence to:* Alexander Gelfan (hydrowpi@iwp.ru)

9 **Abstract.** A long-term forecasting ensemble methodology, applied to water inflows into the Cheboksary reservoir, is
10 presented. The methodology is based on a combination of semi-distributed hydrological model ECOMAG that allows for
11 calculation of an ensemble of inflow hydrographs using two different sets of weather ensembles for the lead-time period: the
12 observed weather data constructed on the basis of the Ensemble Streamflow Prediction methodology (ESP-based forecast),
13 and the synthetic weather data simulated by a multi-site weather generator (WG-based forecast). We have studied: (1)
14 whether there is any advantage of the developed ensemble forecasts in comparison with the currently issued operational
15 forecasts of water inflow into the Cheboksary reservoir, and (2) whether there is any noticeable improvement in a
16 probabilistic forecasts when using the WG-simulated ensemble compared to the ESP-based ensemble? We have found that
17 for 35-year period beginning from the reservoir filling in 1982, both continuous and binary model-based ensemble forecasts
18 (issued in deterministic form) overperform the actually used operational forecasts of the April-June inflow volume and,
19 additionally, provided acceptable forecasts of water regime characteristics other than inflow volume. We have also
20 demonstrated that the model performance measures (in verification period) obtained from the WG-based probabilistic
21 forecasts which are based on a large number of possible weather scenarios, appeared to be more statistically reliable than the
22 corresponding measures calculated from the EPS-based forecasts based on observed weather scenarios.

23 1 Introduction

24 Spring freshet is a hydrological phenomenon, which magnitude is highly dependent on the amount of water accumulated in
25 surface and subsurface storages of the river basin during several months prior to the snowmelt. This dependency serves as a
26 physical basis to predictability of spring runoff (Li et al., 2009). As stated by Lettenmaier and Waddle (1978, p.1) “snowmelt
27 runoff is one of the few natural phenomena for which relatively accurate long-term forecast can be made”.

28 Implementation of this opportunity is crucial for the water reservoirs of the Volga-Kama Reservoir Cascade (VKRC) – one
29 of the world’s largest multi-purpose water management systems. The VKRC is located within the largest European Volga

1 River basin (area of 1 350 000 km²) and consists of 11 reservoirs that hold from 1 to 58 km³ of water and conduct seasonal
2 and multiyear flow regulation. The VKRC was designed to redistribute the highly uneven runoff of the Volga River, with 2/3
3 of the annual runoff volume occurring during the two to four months of the spring-summer freshet. This task, aimed at
4 optimizing reservoir management for power production, navigation and flood protection, is even more complex due to the
5 requirement of annual spring water release to Lower Volga aimed at allowing for sturgeon spawning. Such several-weeks-
6 long regulated release with predefined amount and temperature of water during the spring freshet is a unique task for a water
7 management system (Avakyan, 1998). Hence, a reliable and forehand forecast of snowmelt inflow into the VKRC reservoirs
8 is crucial for the decision makers.

9 By the mid-1960s, the specific methods were developed, which underlie the contemporary operational forecast for VKRC
10 management (water supply forecast). For different reservoirs, the produced forecasts are based on two primary techniques:
11 the index methods, and the so-called physical-statistical methods (Gelfan and Motovilov, 2009; Borsch and Simonov, 2016).
12 Both methods produce deterministic (despite the term “physical-statistical”), purely data-driven forecasts and relate the
13 predictors (such as initial snow water equivalent, soil freezing and soil moisture indices, precipitation amount for the forecast
14 period) to the main predictand - the spring inflow into a reservoir. The initial basin characteristics are derived from
15 observations, yet the precipitation amount is typically set to the climatic mean. The operational water supply forecasts
16 methodology is used in real practice by water managers and remains unchanged over the past half-century.

17 While the utility of data-driven flow forecasts (which currently may be based on advanced statistical and machine learning
18 techniques) has been demonstrated on various examples (see, e.g. Abrahart et al., 2012), their skill and reliability depend on
19 the amount and stationarity of available data and are not always adequate. The forecast improvement could not be expected
20 within the framework of the purely data-driven approach because of reduction of the observational network in the Volga
21 basin (estimated at 30% in (Borsch and Simonov, 2016)), non-homogeneity of the observations caused by changes in the
22 measurement techniques, changes in climate, land use and so on.

23 An opportunity to improve the operational water supply forecasts of water inflow into VKRC lies in shifting from the
24 traditional exclusively data-driven forecasts towards hydrological model-based forecasts, and from deterministic
25 methodology to the one using ensembles with a possibility to characterise forecast uncertainty. During the last 20-30 years
26 there have been a general understanding of the necessity of such a shift to ensemble streamflow prediction (ESP) systems
27 (e.g., Day, 1985), and a considerable research effort in this direction (Franz et al., 2003; Wood and Lettenmaier, 2006; Li et
28 al., 2009; Shukla and Lettenmaier, 2011; Yossef et al., 2013; Najafi and Moradkhani 2015; Demirel et al. 2015; Beckers et
29 al. 2016; Arnal et al., 2017; Mendoza et al. 2017). Such systems are currently used more and more in operational mode by
30 national weather services in the Untied States (e.g. McEnery et al., 2005), Canada (Druce, 2001) and other countries
31 (Pappenberger et al., 2016).

1 In its original form, an ESP is based on an assumption that historical time series of observed meteorological variables are
2 representative for a local climate. These series are used as an ensemble of meteorological inputs into a hydrological model to
3 simulate corresponding ensembles of streamflow forecasts. This allows for considering uncertainty in weather conditions
4 during the forecast horizon and provide an opportunity to quantify the corresponding uncertainty (and hence, risk) in the
5 forecast-based decision support systems for reservoir management. In addition, utilizing the process-oriented hydrological
6 models results in increasing the physical adequacy of forecasts and, potentially, in improving forecast accuracy in
7 comparison with the methods currently used in operational practice. However, such quantitative comparisons is not a
8 common place; to our knowledge the only example is the comprehensive experiment presented by Mendoza et al. (2017) and
9 comparing the ESP model-based forecasts with the operational data-driven forecasts for a multi-year historical period.

10 The observed weather scenarios that are used within the ESP framework do not encompass all of the possible weather
11 conditions for the forecast period. It is desirable to account not only for the observed weather, but for possible weather
12 condition that might lead to freshet events of rare occurrence. Assessing the magnitude of such an event might be crucial for
13 decision making. Moreover, hence the ensemble size is limited to the number of the historical years, statistical problems can
14 appear stemming from large sample errors. For instance, Buizza and Palmer (1998) demonstrate improvement of the weather
15 forecast skill as the ensemble size increases, wherein degree of improvement depends on the verification measure used.
16 Particularly, the ranked probability skill score is strongly dependent on ensemble size and negatively biased (see also Müller
17 et al. 2005, Weigel et al., 2007). Different aspects of the ensemble size effect on statistical properties of the ensemble
18 weather forecast and verification scores are studied by Richardson (2001), Ferro et al. (2008), Najafi et al. (2012). The
19 problem can be solved by incorporating synthetic, stochastically generated time series of weather variables instead of the
20 historical data used within the ESP framework. As a result, hydrological system response to a large variety of possible
21 weather conditions can be reproduced and large ensemble of forecasts can be predicted.

22 There are not too many attempts to use stochastic weather generator (WG) within framework of long-term ensemble
23 forecasting. Hanes et al. (1977) were probably the first who used Monte-Carlo simulated sequences of daily precipitation to
24 drive the conceptual US Geological Survey hydrological model and provide ensemble seasonal forecast of snowmelt runoff
25 volume. A physically-based distributed hydrological model was used in combination with a weather generator to create a
26 long-term probabilistic forecast of spring runoff of rivers in Central Russia in Kuchment and Gelfan (2007), Gelfan et al.
27 (2015). Caraway et al. (2014) incorporated a stochastic weather generator into the ESP to make a probabilistic seasonal
28 climate forecasts and applied the modified methodology to the San Juan River snowmelt dominated basin. Beckers et al.
29 (2016) used ENSO-conditioned weather generator to compensate for the reduction of ensemble size in the post-processing
30 ensemble forecast scheme presented for the Columbia River basin.

31 The studies and examples mentioned above serve as the background and the main motivation for this study. The objective of
32 this study is to contribute to the EPS-related studies, with the focus on the comparative analysis between the data-driven
33 techniques used in operational forecasts, and the ensemble forecasts of streamflow, using two different weather scenarios: a)

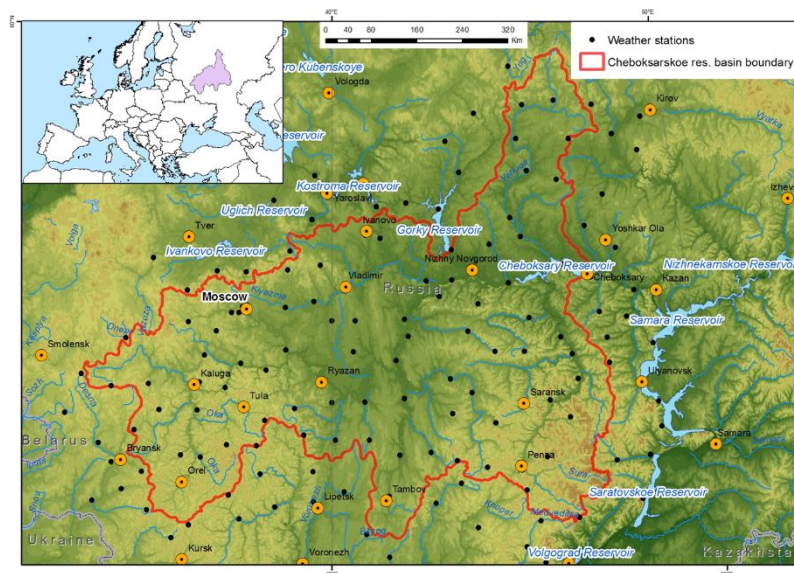
1 based on the historical data, and b) employing the WG-based forecasts. The case study is the Cheboksary reservoir of the
2 VKRC cascade for which the operational forecasts are available since 1982.

3 Thus, this study is an attempt to answer the following two research questions: (1) Does the model-based ensemble
4 methodology allow one to improve reliability and skill of the operational forecast of spring inflow into the Cheboksary
5 reservoir, and to what extent? (2) Does the enlarged ensemble size lead to any noticeable advantage when using the WG-
6 simulated ensemble compared to the ESP-based ensemble?

7 The remaining part of this paper is organized as follows. The case study is described in the next section. The operational
8 forecast methodology, as well as the proposed forecasting approach including modelling tools (hydrological model and
9 stochastic weather generator), forecasting schemes, experimental design and forecast verification measures are described in
10 Section 3. Results and discussion are presented in Section 4. The overall conclusions and recommendations are given in
11 Section 5.

12 2. Case study basin

13 The Cheboksary reservoir is located on the Volga River in central part of the European Russia. It was constructed in 1982 to
14 become the 11th member of Volga-Kama reservoir cascade with Nizhegorodskoe reservoir upstream and Kujbysevskoe
15 reservoir downstream of it. Total unregulated basin area of the Cheboksary reservoir is 373 800 km² (Fig. 1). Its main
16 tributaries - Oka, Sura and Vetluga Rivers - account for 80 to 90% of annual inflow into the reservoir.



17
18 **Figure 1: Cheboksary reservoir basin: topography, river network, weather stations**

19 Local climate conditions can be described as moderately continental, with cool snow-abundant winter and relatively hot
20 summer. Mean annual temperature ranges from 1.4°C in the northern part of the basin to 4.8°C in the southern part. During

1 wintertime air temperature may fall as low as -35 - -40°C. Annual precipitation amount ranges between 650 and 750 mm
 2 throughout the territory. Around 60% of the precipitation occurs as rain. Most of winter precipitation is stored as snow cover,
 3 emerging in mid-December and lasting until mid-April. Snow water equivalent ranges from 50 mm in the South-Western
 4 part up to 100 – 120 mm in the North. Springtime snowmelt contributes to high-flow freshet – the dominating hydrological
 5 season accounting for around 65% of the total annual inflow into the reservoir (51.3 km³). Typically, freshet commences
 6 around mid-April and lasts until June. Mean volume of inflow for the period of reservoir operation (1982-2016) is 33.4 km³,
 7 mean maximum inflow discharge is 9355 m³/s.

8 **3. Method**

9 **3.1 Operational data-driven forecast of spring inflow into the Cheboksary reservoir: a current practice**

10 Methodology for forecasting the spring inflow into the Cheboksary reservoir was developed by E.P. Chemerenko (1992) on
 11 the basis of so-called physical-statistical approach originally proposed for the reservoirs of Middle Volga in mid-1960s
 12 (Zmieva, 1964; Gelfan and Motovilov, 2009). This approach is currently in use by the Russian Hydrometeorological service
 13 (Roshydromet) for inflow forecasting into all reservoirs located on the Middle Volga River.

14 Water inflow volume Y into the Cheboksary reservoir is forecasted according to the equation:

$$15 \quad Y = \sum_{i=1}^5 \alpha_i y_i + \beta \quad (1)$$

16 where y_i is the runoff forecast at streamflow gauge i , located on the reservoir tributaries: $i=1$ – Oka River, Polovskoe gauge
 17 (drainage area $F=99000$ km²), $i=2$ – Klyazma River, Kovrov gauge ($F=24900$ km²), $i=3$ – Vetluga River, Vetluzhsky gauge
 18 ($F=27400$ km²), $i=4$ – Sura River, Poretsky gauge ($F=50100$ km²), $i=5$ – Tsna River, Knyazhevo gauge ($F=13600$ km²), α_i ,
 19 β – regression coefficients estimated from the streamflow data observed at the corresponding gauge.

20 The runoff volume y_i at i th gauge is forecasted by a unified procedure. The predictors are: basin averaged snow water
 21 equivalent (S , mm), soil freezing depth, (FD, cm), soil moisture index (W , dimensionless) on a forecast issue date, and total
 22 precipitation (x , mm) during the forecast horizon.

23 Runoff volume at each gauge is calculated as follows:

$$24 \quad y = (1 - f) \left\{ (S_1 + x) - P_0 \left[1 - \exp \left(\frac{S_1 + x}{P_0} \right) \right] \right\} + f\eta(S_2 + x) \quad (2)$$

$$25 \quad P_0 = a \exp \left[-b(\theta - \theta_{\min})^c \right] \quad (3)$$

26 where S_1 , S_2 are the snow water equivalent at the forecast issue date within the deep frozen ($FD \geq 60$ cm) and non-deep frozen
 27 ($FD < 60$ cm) parts of the river basin, respectively, derived from snow observations; x is the total precipitation for the forecast

1 horizon, assigned as climatic mean; f is the fraction of the basin area covered by deep-frozen soil, derived from soil freezing
2 observations; θ is the soil moisture index, calculated from precipitation amount during the preceding autumn period; η is
3 the runoff coefficient from the basin fraction with non-deep frozen soil calculated as a function of θ ; a , b , c , θ_{\min} are the
4 parameters derived from hindcasts for the 30-year period before the reservoir filling in 1982.

5 The operational forecast of water inflow volume into the Cheboksary reservoir for April-June period is issued just before the
6 beginning of this period (March 27) and then updated 2-3 times during April-May. In this paper, the operational
7 deterministic forecast (not updated, i.e. issued before the beginning of April) is compared with the deterministic forecast
8 derived from the model-based ensemble forecasts described below.

9 **3.2 Model-based ensemble forecast technique and verification measures**

10 **3.2.1 Modelling tools**

11 *Hydrological model*

12 The ECOMAG (ECOLOGical Model for Applied Geophysics) is a semi-distributed process-based hydrological model
13 describing snow accumulation and melt, soil freezing and thawing, water infiltration into unfrozen and frozen soil,
14 evapotranspiration, thermal and water regime of soil, overland, subsurface and channel flow on a daily time step (Motovilov
15 et al., 1999). The model accounts for measurable watershed characteristics such as surface elevation, slope, aspect, land
16 cover and land use, soil and vegetation properties. The parameters are spatially distributed by partitioning the watershed into
17 sub-basins (elementary basins). Parameterization of the sub-grid processes is described by Motovilov (2016). The model is
18 driven by time series of daily air temperature, air humidity and precipitation intensity.

19 The model was earlier applied for hydrological simulations in many river basins with highly varying sizes and characteristics
20 - from small-to-middle size European basins (Gottschalk et al., 2001) to the large Volga, Lena, Mackenzie with watershed
21 areas exceeding a million km² (Motovilov 2016; Gelfan et al., 2017).

22 In this study, 1x1 km spatial resolution DEM was used for the basin discretization and river network construction. A total of
23 1045 elementary basins were delineated, with average area of 340 sq. km. The model forcing data for each elementary basin
24 were interpolated from the 157 weather station data (see Fig. 1) employing the inverse-distance method. Most parameters are
25 physically meaningful and were derived through available measurements of the basin characteristics (topography, soil and
26 vegetation properties).

27 The model was calibrated and validated against the Cheboksary reservoir daily water inflow observations beginning from
28 January, 1, 1982 (the 1st year after the reservoir filling to capacity) to December 31, 2016: calibration covered the period of
29 2000-2010, the rest of the data were used for the model evaluation. The ECOMAG calibration procedure is described in
30 detail by Gelfan et al. (2015). Here, we emphasize the two issues concerning this procedure. First, the values of several key

1 parameters pre-assigned from literature or from the available measurements are considered as the initial approximations of
2 the optimal values and the latter are sought within the neighborhood of the initial, pre-assigned values. Second, during the
3 calibration process, the ratios between the initial values of the distributed parameter corresponding to different soils,
4 landscapes and vegetation are preserved. The Nash and Sutcliffe (1970) efficiency criterion NSE is adopted to represent the
5 goodness of fit of the simulated and measured variables.

6 *Multi-site weather generator (MSFR_WG)*

7 The Multi-Site FRagment-based stochastic Weather Generator (MSFR_WG) is the stochastic model using Monte-Carlo
8 simulation to generate time-series of daily weather variables (precipitation, air temperature and air humidity deficit),
9 retaining statistical properties, both spatial and temporal, of the corresponding observed variables. This modeling procedure
10 is based on the so-called “spatial fragments’ (SFR) resampling method” initially presented by Gelfan et al (2015). The SFR-
11 method is a modification of the temporal fragments’ (TFR) method proposed by Svanidze (1980) for stochastic simulation of
12 highly autocorrelated time-series.

13 The SFR resampling method includes the following steps:

- 14 1. Computation of N normalized fields (“spatial fragments”, SFR) of weather variables on the basis of the available
15 meteorological data. SFRs are computed for each of N years of observations by dividing each daily value of the
16 specific variable by the corresponding spatially averaged annual value.
- 17 2. Monte-Carlo simulation of synthetic time-series of M spatially averaged annual weather variables reproducing
18 temporal statistical features of the corresponding annual variables derived from observation data. Cross-correlation
19 between annual values of the simulated weather variables is taken into account through the Cholesky's
20 decomposition method (see e.g. Press et al., 2007).
- 21 3. Calculation of the synthetic daily fields of weather variables by multiplying the computed SFRs (see step 1) on the
22 Monte-Carlo simulated spatially averaged annual value of the corresponding variables (see step 2). SRFs are
23 randomly chosen from the available set by the Latin Hypercube method (McKay et al., 1979).

24 The advantage of MSFR_WG is that it has a small number of free parameters in comparison with the widely used multi-site
25 weather generators (see, e.g. Khalili et al. (2011) and references therewith), and does not require complex estimation
26 procedures. Such features typically indicate that the model has high robustness.

27 **3.2.2 Ensemble forecasting technique**

28 The proposed ensemble forecasting procedure utilized in this study was verified by producing hindcasts of water inflow into
29 the Cheboksary reservoir from the 1st of April for 3 months ahead (up to 30th of June). The hindcasts cover a 35-year period

1 between 1982 and 2016. (Hereafter, we use the term “forecasts” for these hindcasts). For each i -th year of the verification
2 period ($i=1, 2, \dots, 35$), the procedure includes the following steps:

- 3 (1) Spin-up ECOMAG-based simulations (“warm start”) using meteorological observations data prior to the
4 forecast issue date (March, 31) in order to calculate the initial watershed hydrological state (soil, snow and
5 channel water contents, groundwater level, soil freezing depth, etc.) that initializes the forecast. The
6 simulations start from the end of the previous freshet, i.e. 8-9 months before the forecast issue date;
- 7 (2) Selection of a weather scenario¹ from the N_{EPS} -member ensemble of the observed weather or from the N_{WG} -
8 member ensemble of the generated weather for the forecast horizon;
- 9 (3) Simulating daily inflow hydrograph by the ECOMAG model driven by the selected scenario;
- 10 (4) Repetitive selection of the next weather scenario (step 2) from the ensemble and calculation of the
11 corresponding inflow hydrograph (step 3). The corresponding ensemble of N inflow hydrographs is formed (N
12 $=N_{EPS}$ or $N=N_{WG}$);
- 13 (5) From each of the modelled hydrographs, the following inflow characteristics are derived: (1) inflow volume
14 (hereafter referred to as W), (2) maximum inflow discharge (Q_{max}), (3) number of days with the inflow
15 discharge above the mean observed discharge for the forecast horizon (N_q), (4) number of days with the inflow
16 discharge above the mean maximum observed discharge for the forecast horizon (N_{qMax}).
- 17 (6) Deterministic (ensemble mean) and probabilistic forecast are derived and verified for each of the inflow
18 characteristics.

19 3.2.3 Verification measures

20 To verify deterministic and probabilistic model-based forecasts, as well as to compare them with each other and with the
21 operational data-driven forecast of water inflow into the Cheboksary reservoir, we used the following, quite traditional,
22 measures of the forecasts’ efficiency and skill.

23 For the deterministic forecast verification, we used the mean error (ME), relative bias (BIAS), root-mean-squared error
24 (RMSE), and Pearson’s correlation coefficient R . In addition, for presentation, we used the Taylor diagram (Taylor, 2001)
25 which combines three forecast characteristics in one chart, namely the forecast standard deviation, RMSE and the correlation
26 coefficient between the observations and the forecasted values.

¹ Hereafter, by “weather scenario” we mean an array of weather time-series (daily precipitation amount, air temperature and humidity deficit) that are used to drive the hydrological model for the forecast horizon

1 For categorical forecast verification, we used measures that can be calculated from a contingency table (Ferro and
2 Stephenson, 2011), such as probability of detection (POD, shows the correct forecast fraction of the observed events), false
3 alarm ratio (FAR, shows the fraction of forecasts that did not occur), frequency BIAS (shows correspondence of the
4 observed and the forecasted events), Heidke skill score (HSS, shows the advantage of the forecast as compared to a random
5 forecast), Hanssen and Kuipers score (KSS, can detect if the forecast is hedging) and Symmetric Extremal Dependency
6 Index (SEDI, evaluates the performance of the forecast of rare binary events).

7 The probabilistic ensemble forecasts performance was assessed by several verification measures. The ability of forecasts to
8 correctly predict the category of the event occurred within several categories was measured by Ranked Probability Score
9 (RPS) (Wilks, 1995) that can also be treated as the mean squared error of the probabilistic forecast. The probability forecast
10 efficiency relating to streamflow climatology was measured by the Ranked Probability Skill Score (Wilks, 1995). To
11 visualize the specifics of probabilistic forecasts, three diagrams were employed. The predictive Q-Q plot (Laio and Tamea,
12 2007) was used to assess the degree of correspondence between the cumulative distribution function of predictions and the
13 observed values. The reliability diagram (Hartmann et al., 2002) was used to plot the forecast probability against the relative
14 frequency of the observations in the corresponding forecast probability bin. Finally, the discrimination diagram (Wilks,
15 1995) was used to show the frequency of each forecast probability for events and non-events.

16 Full list of the aforementioned verification measures, their formulations, units, and value ranges are presented in Table 1S
17 (Suppl. Materials)

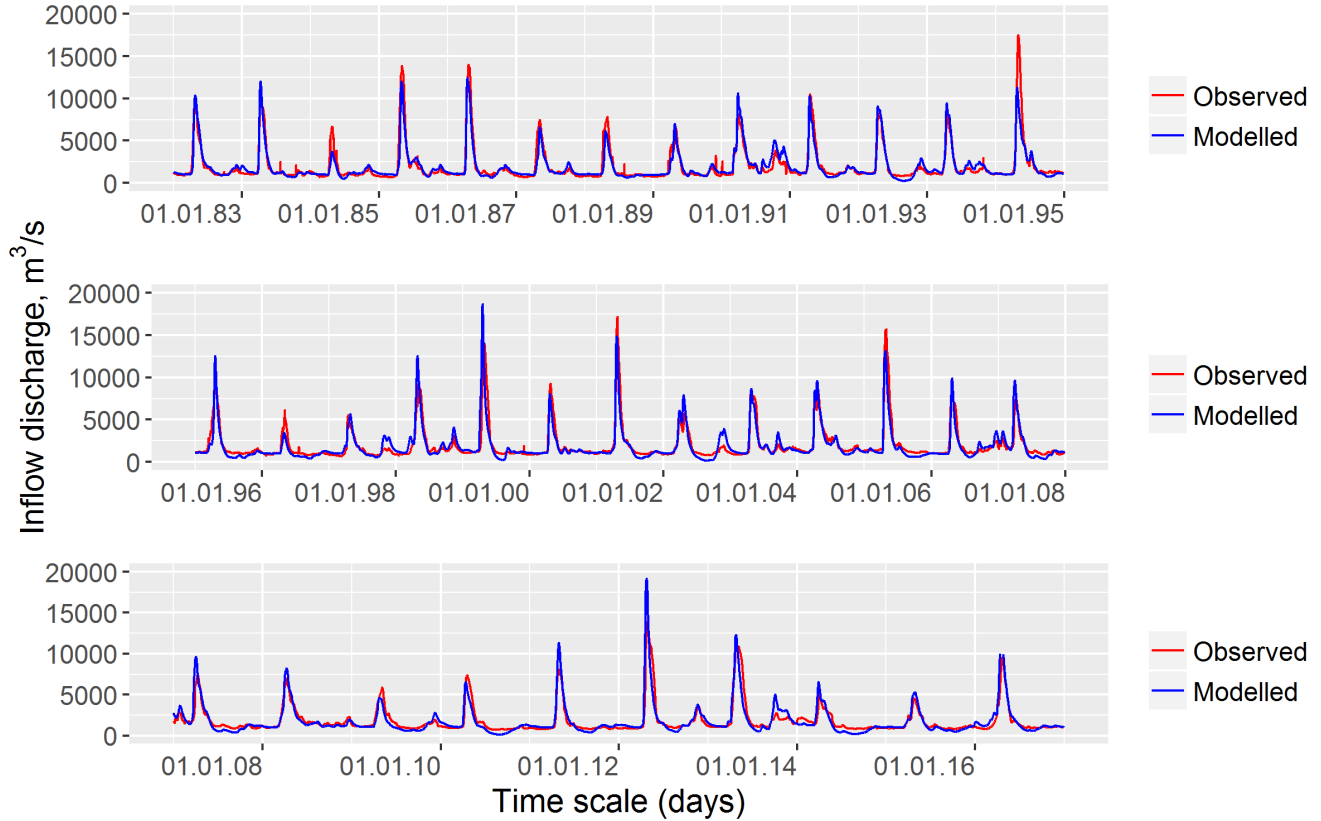
18 **4. Results and discussion**

19 **4.1 Calibration and evaluation of the hydrological model**

20 The hydrological model was calibrated and evaluated against the daily time-series of water inflow into the Cheboksary
21 reservoir for the periods of 2000-2010 and 1982-1999, 2011-2016, respectively. The observed inflow data do not account for
22 inflow from the upstream Nizhegorodskoe reservoir. Fig. 2 compares hydrographs of the observed and the simulated daily
23 inflow discharges. Nash-Sutcliffe efficiency for daily inflow discharge is rather high (NSE=0.80) and ranges from 0.79 for
24 the evaluation period to 0.83 for the calibration one. One can see that the model demonstrates good performance with
25 respect to this criterion. Additionally, a small difference between the criteria estimated for the calibration and evaluation
26 periods confirms the model robustness (Gelfan et al., 2015).

27 The model performance was tested also by comparison of the observed and simulated inflow characteristics, which were
28 used then for the forecast verification and listed in sub-section 3.2.2. Figure 3 shows scatterplots of the observed and
29 simulated characteristics of the inflow into the Cheboksary reservoir in April – June. In general, the inflow volume is well
30 simulated, yet slightly underestimated for the high flows (above 50 km³, see Fig. 3a). Maximum inflow discharge is a highly
31 uncertain characteristic, but is still well simulated by the model (Fig. 3c). The number of days above a certain inflow

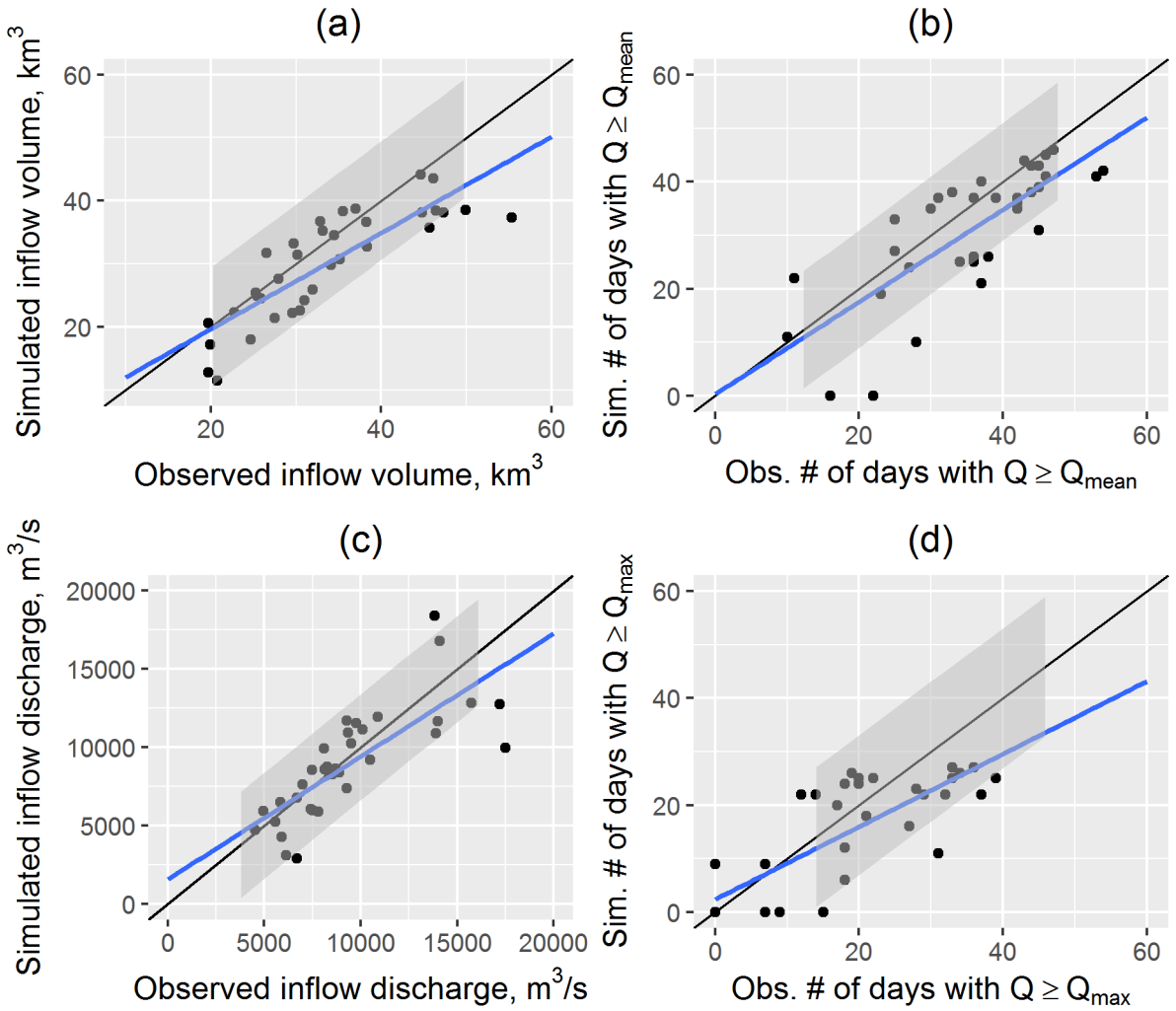
1 discharge threshold is a highly important characteristic for various users, e.g. waterways navigation and water supply. For
 2 the number of days above long-term (1982-2016) mean inflow discharge during the period between April and June, the
 3 model shows less days than the observed ones (Fig. 3b) – 31 against 36 days, on average for the whole period. For the
 4 number of days above long-term mean maximum inflow discharge the model also shows less days (Fig. 3d) – 13 against 17
 5 days, on average.



6
 7 **Figure 2: Observed and simulated daily discharge of inflow into the Cheboksary reservoir**

8 Relative bias (BIAS) of the inflow volume in April – June for the whole period 1982 – 2016 is BIAS=-3%; RMSE of the
 9 inflow volume (5.23 km^3) consists 55% of the observed data standard deviation ($\sigma_w=9.41 \text{ km}^3$). Relative bias of the
 10 maximum inflow discharge BIAS=5% m^3/s ; RMSE=2321 m^3/s , that is 30% lower than the standard deviation of the
 11 observed maximum inflow discharge ($3385 \text{ m}^3/\text{s}$).

12 The obtained results allow us to conclude that the developed model can be considered as a suitable tool for the long-term
 13 hydrological forecast of spring water inflow into the Cheboksary reservoir.



1

2 **Figure 3: Scatterplots for the observed and simulated characteristics of inflow into the Cheboksary reservoir during April – June:**
 3 **volume W (a), maximum discharge Q_{max} (c), number of days above mean inflow discharge N_q (b), number of days above mean**
 4 **maximum inflow discharge $N_{q\text{Max}}$ (d) Blue line represents linear fit. Grey shaded area denotes variance band of ± 1 standard**
 5 **deviation of the respective observed values**

6 **4.2 MSFR_WG: parameter estimation and model testing**

7 Time series of daily precipitation, air temperature and humidity deficit observed at the meteorological stations located at the
 8 Cheboksary reservoir basin for 51 years (1966-2016) are used to estimate the nine parameters of the developed stochastic
 9 model. The parameters estimated by the method of moments are shown in Table 2S in the Supplementary Materials. The
 10 stochastic models were comprehensively tested through their ability to reproduce the main statistical characteristics of
 11 meteorological processes at the Cheboksary reservoir basin. For testing, we compared only those characteristics of the
 12 observed and simulated time-series, which are neither the parameters of the model nor a single-valued function of the

1 parameters as suggested in Gelfan (2010). Statistics of the 1000-member Monte-Carlo generated ensemble of daily
 2 meteorological variables were compared with the following corresponding statistics derived from observations: mean and
 3 variation of annual and monthly values, autocorrelation functions of daily and monthly values of the specific variables.
 4 Results demonstrating comparison between statistical properties of the observed and simulated series are shown in
 5 Supplementary Materials for spring months and for several selected stations (Figs. 1S-8S).

6 4.3 Forecast verification

7 4.3.1 Ensemble (model-based) and operational (data-driven) deterministic forecasts

8 We verified the two types of the ensemble forecasts (ESP-based and WG-based), compared them with each other and with
 9 the operational forecasts of water inflow into the Cheboksary reservoir for April-June 1982-2016. To make a deterministic
 10 forecast, the forecasted inflow characteristics were averaged over the corresponding ensembles (51-member in the case of
 11 the ESP-based forecast and 1000-member for the WG-based forecast) to produce a single-value forecast of the desired
 12 characteristic: W , Q_{max} , N_q , N_{qMax} . Operational forecasts of inflow volume for the same April-June periods of 1982-2016 were
 13 obtained from the official Roshydromet forecast bulletins (reports). All forecasts were analyzed to assess the forecast
 14 performance measures: mean absolute error, BIAS, and RMSE. The results are presented in Table 1.

15 **Table 1 – Statistics of the operational (op.) and the ensemble (ESP and WG) deterministic forecasts of inflow into the Cheboksary**
 16 **reservoir for April-June in 1982-2016**

Inflow characteristics	Obs.	Mean			Mean error			BIAS*			RMSE		
		Op.	ESP	WG	Op.	ESP	WG	Op.	ESP	WG	Op.	ESP	WG
W, km³	33.4	32.9	32.3	33.5	-0.5	-1.1	0.1	-1%	-3%	0%	6.52	5.06	5.19
Q_{max}, m³/s	9355	N/A	9463	9958	N/A	108	603	N/A	1%	6%	N/A	1970	2244
N_q, days	35.9	N/A	35.9	36.1	N/A	0	0.2	N/A	0%	1%	N/A	8.0	8.8
N_{qMax}, days	17.0	N/A	16.2	17.1	N/A	-0.8	0.1	N/A	-5%	1%	N/A	7.4	8.2

17 *The measure abbreviations are defined in Table 1S

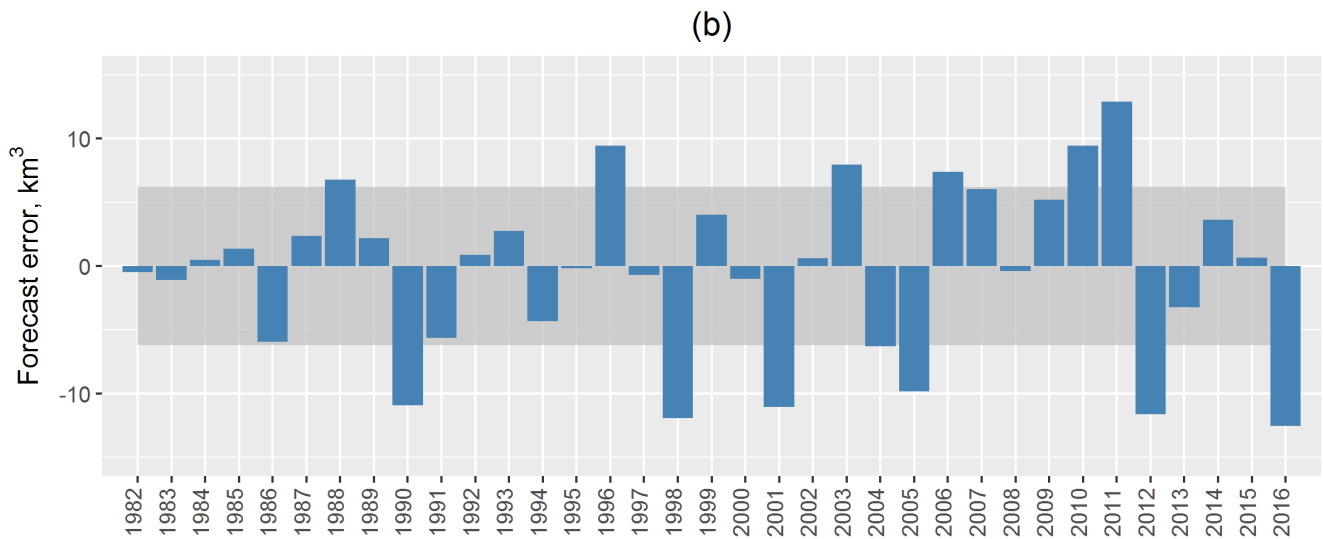
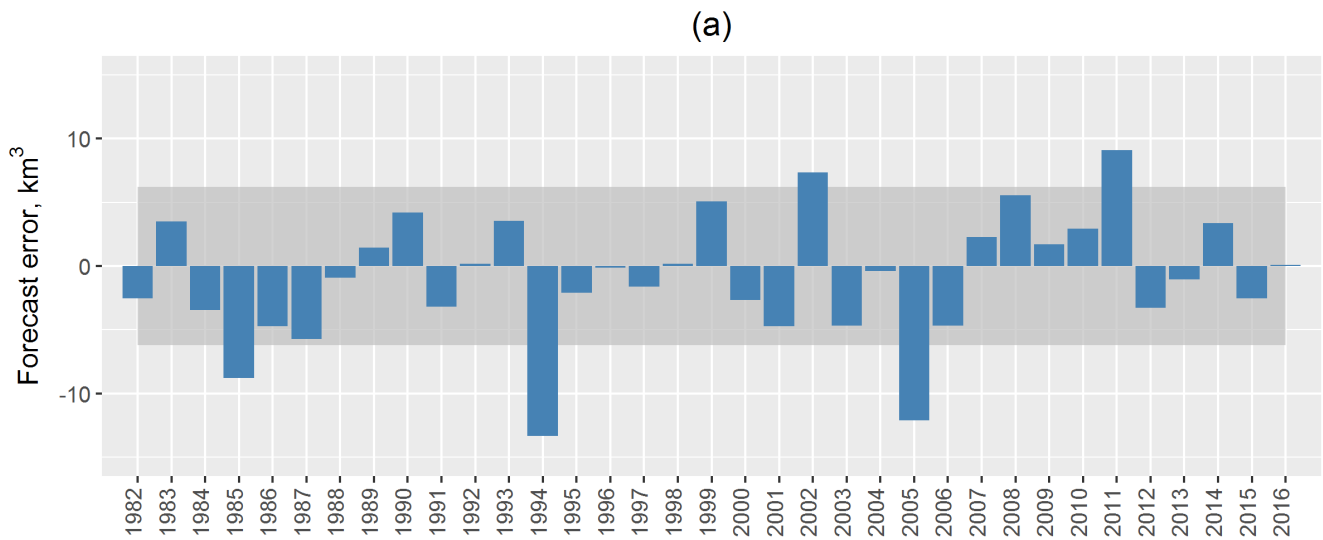
18 First, the deterministic forecasts of the inflow in April-June were compared to the operational forecasts for 1982-2016. As
 19 shown in Table 1, the mean error of the operational forecasts appeared to be quite low (around 1%) and close to those of the
 20 ESP and WG ensemble average values. However, the operational forecasts RMSE values are significantly higher than those
 21 of the ESP and WG forecasts and accounts for almost 70% of the observed inflow volume variability $\sigma_w=9.61 \text{ km}^3$. For the
 22 ESP and WG-based forecasts these values are around half of σ_w .

23 Fig. 4 compares the inflow volume forecast errors of the operational forecasts (Fig. 4a) with the ESP-based forecast errors
 24 (Fig. 4b). The shaded area in the figures represents the area of the acceptable error $[-0.674\sigma_w; 0.674\sigma_w] = [-6.48 \text{ km}^3; 6.48$

1 km³]. In the Russian operational forecasting practice, a forecast is considered acceptable if its error falls into this area, and
2 the forecast acceptability is calculated as the ratio of the acceptable forecasts to the whole number of forecasts. According to
3 the assumption of the Gaussian distribution of the forecast errors, 50% of the forecasts by climatology should fall into this
4 interval. It can be seen from Fig. 4 that five of 35 ESP-based forecasts (in 1985, 1994, 2002, 2005 and 2011) and every third
5 (12 of 35) operational forecasts were not acceptable, i.e. the ESP-based forecast acceptability is 89% and that of the
6 operational forecast is 66%. Note that the unacceptable forecasts in both cases occurred in the years with spring precipitation
7 amount significantly differing from the corresponding climatic mean.

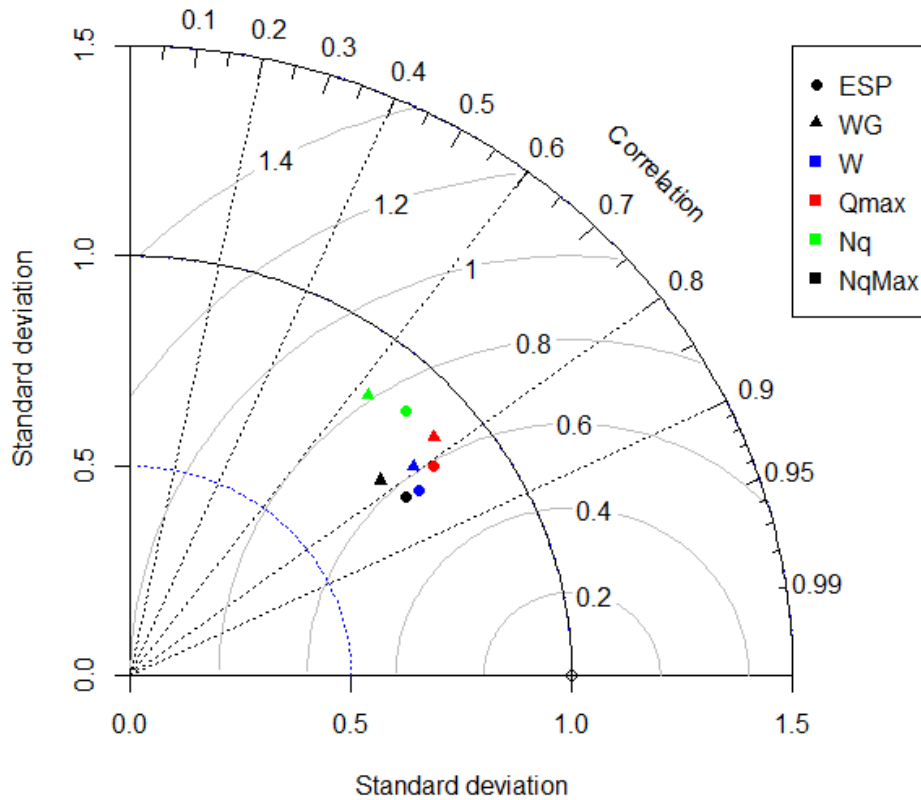
8 To compare the ESP-based and the WG-based forecasts, we present them in the form of the Taylor diagram (Fig. 5; Taylor,
9 2001), which combines three forecast characteristics in one chart, namely, the forecast standard deviation, RMSE and the
10 correlation coefficient between the observed and the forecasted values of the inflow characteristics. The values of all
11 characteristics are normalized by dividing the RMSE by the standard deviation of the observations. This normalization
12 provides a demonstration of the forecast efficiency expressed in fractions of the observed standard deviation. As long as the
13 forecast RMSE is less than the standard deviation of the observations, the forecast can be considered efficient against
14 climatology.

15 It can be seen from Fig. 5 that the ESP-based forecasts of W , Q_{max} and N_{qMax} are slightly better correlated with the
16 observations than the WG-based forecasts. Pearson's R values of the ESP-based forecasts are over 0.8 for all characteristics,
17 except for N_q . Forecasts of N_q are less correlated with the observations, with values of R for ESP-based and WG-based
18 forecasts equal 0.73 and 0.63, respectively. Forecasts of Q_{max} and N_{qMax} show normalized RMSE values around 58-67% of
19 the standard deviation of the corresponding observed characteristics.



1

2 **Figure 4: Errors of the ESP-based (a) and operational (b) forecasts of the April-June volume of water inflow into the Cheboksary**
 3 **reservoir. (Solid lines present boundaries of the acceptable error equaled $\pm 0.674\sigma_w$, where $\sigma_w=9.61 \text{ km}^3$ is the standard deviation**
 4 **of the observed inflow volume)**



1

2 **Figure 5: Taylor diagram of ESP (circle) and WG-based (triangle) forecasts of inflow volume W (in blue), maximum inflow**
 3 **discharge Q_{max} (red), number of days with inflow discharge above mean N_q (green), number of days with inflow discharge above**
 4 **maximum N_{qMax} (black).**

5 For the purpose of reservoir management, it is often crucial to determine whether the expected inflow characteristic will
 6 exceed the corresponding mean value. To verify the methodology capability of predict this exceedance, the observations and
 7 forecasts were converted into binary vectors with “zero” value representing the event of non-exceedance of the mean annual
 8 value and “one” for the event occurrence. For example, for W , the event occurs with the exceedance of mean inflow volume
 9 during April – June. The forecast binary measures assessed with the use of the contingency tables and described in Table 1S
 10 are shown in Table 2.

11 The forecasts show good detection estimates (even perfect for Q_{max}) for both model-based methodologies. However, as the
 12 frequency Bias is high, this might be the result of overprediction, so with the high values of False Alarm Ratio and Hansen-
 13 Kuipers score. For W and Q_{max} , the forecast accuracy with the Heidke Skill Score (HSS) of around 60% is better than the
 14 accuracy of random chance; this means that the forecast is capable of detecting the occurrence of rare extreme events, which
 15 is shown by high values of the Symmetric Extremal Dependency Index (SEDI). Overall, the presented binary verification
 16 measures demonstrate a slight advantage of the ESP-based forecasts over the WG-based forecasts, though the differences are
 17 not significant.

1 **Table 2 – Verifications measures for the binary forecasts (Cheboksary reservoir, April-June of 1982-2016)**

2

Inflow characteristics	POD*			FAR			Freq. BIAS			HSS			KSS			SEDI		
	$R^{**} \in [0;1];$			$R \in [0;1];$ PFM=0			$R \in (-\infty;+\infty)$			$R \in (-\infty;1];$			$R \in (-1;1)$			$R \in (-1;1)$		
	PFM***=1			PFM=0			PFM=1			PFM=1			PFM=1					
	Op.	ESP	WG	Op.	ESP	WG	Op.	ESP	WG	Op.	ESP	WG	Op.	ESP	WG	Op.	ESP	WG
W, km³	0.69	0.87	0.87	0.31	0.24	0.29	1.31	1.13	1.27	0.42	0.66	0.55	0.42	0.67	0.57	0.57	0.82	0.73
Q_{max}, m³/s	N/A	1.00	1.00	N/A	0.33	0.37	N/A	1.50	1.58	N/A	0.66	0.61	N/A	0.74	0.70	N/A	0.93	0.92
N_q, days	N/A	0.77	0.75	N/A	0.23	0.20	N/A	1.00	0.91	N/A	0.39	0.41	N/A	0.39	0.42	N/A	0.53	0.57
N_{qMax}, days	N/A	0.79	0.76	N/A	0.17	0.20	N/A	0.95	0.91	N/A	0.60	0.57	N/A	0.60	0.62	N/A	0.76	0.67

3 *The measure abbreviations are defined in Table 1S

4 ** R is the Range of the measure value

5 *** PFM is the Perfect Forecast Measure value

1
2
3
4
5
6
7
8
9
10
11
12
13
14
15
16
17
18
19
20
21
22
23
24
25
26
27

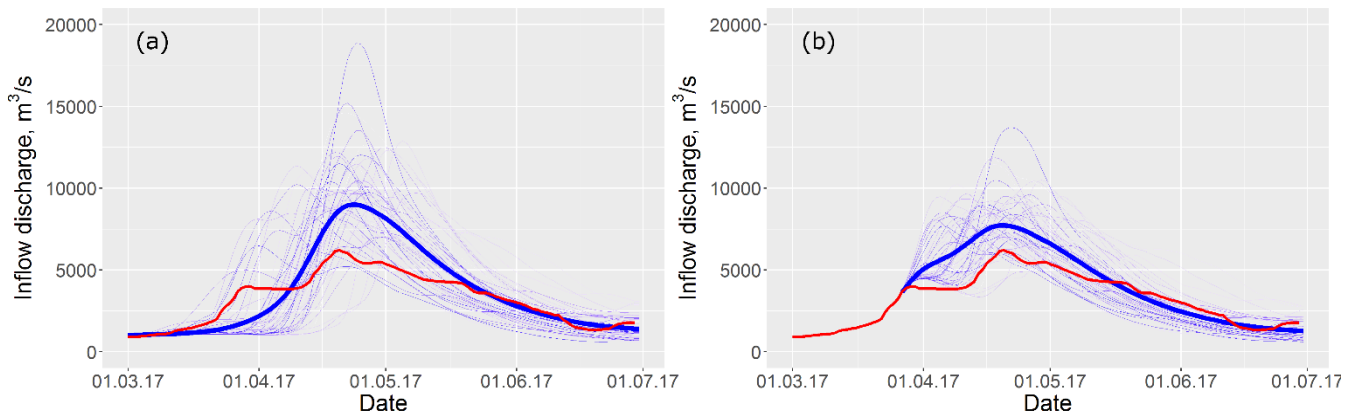
Binary measures of the operational forecasts of inflow volume are worse than those of the model-based forecasts. For instance, only 69% of the observed events (exceedance of mean inflow volume) are correctly forecasted by the current operational methodology and its accuracy relative to that of random chance is less than 50%. An ability of a user to detect rare events on the basis of the operational forecast is also much lower than with the help of ensemble forecasts.

Thus, both continuous (Table 1) and binary (Table 2) model-based forecasts of inflow volume appeared to be more preferable, in general, than the corresponding operational forecasts. However, as one can see from Fig. 4, there were several years, when the operational forecasts were more accurate (in terms of the absolute error) than the ensemble ones. We found that most often the operational forecast outperforms the model-based forecast in those years when the modelled initial snow water equivalent (SWE) on the forecast issue date significantly differed from the observed SWE. Since the latter is the main factor affecting the freshet volume, more accurate (observed) initial snow conditions used in formula (2) resulted in more accurate forecast than the one initiated from the simulated SWE.

4.3.2 Freshet of 2017: testing the ensemble methodology

In the beginning of spring 2017, the basin’s pre-melt conditions were close to climatology: snow water storage was 10 to 15% above the long-term mean value, soil water content and freezing depth were close to the corresponding mean values. However, the weather conditions during the spring freshet formation appeared to be significantly different from climatology. Anomalous warm and sunny weather that settled over the basin in the first half of March has led to commencement of snowmelt and river stage ascent at least half-month earlier than the mean dates. The last decade of March was, on the contrary, cold and damp, and the precipitation amount was twice above normal for this period. As a result, by the end of March the inflow volume (5.13 km^3) into the reservoir exceeded mean March inflow by 32%. Periods of intense snowmelt, interchanged with cold spells and large amount of precipitation, including snowfalls during April and May of 2017 (a number of stations have registered snowfall even in June). Such diversity in weather conditions during the snowmelt period and their difference from the climatology resulted in rather untypical regime of inflow into the Cheboksary reservoir.

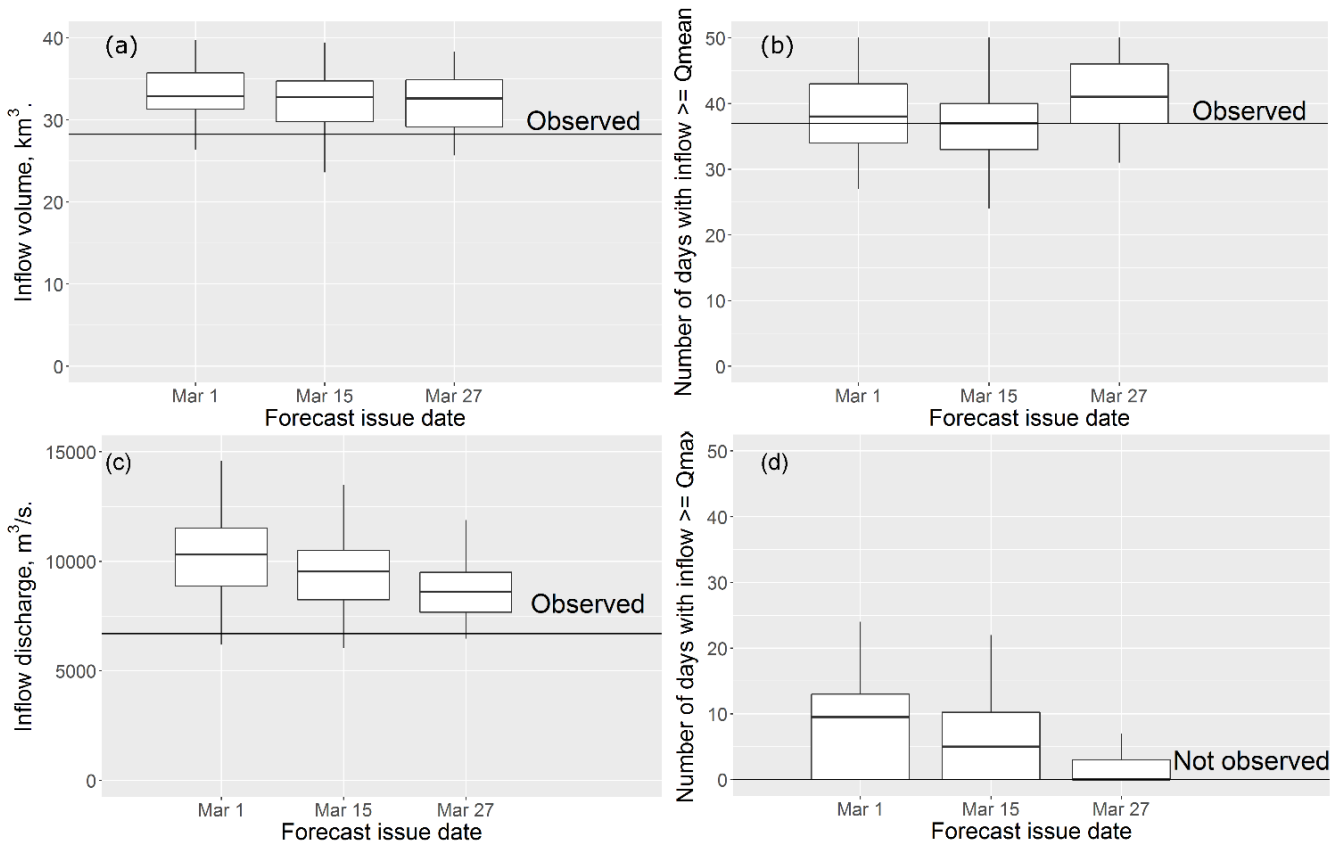
The ESP-based forecasting technique was tested in operational mode during the freshet period of 2017. The forecasts were issued on March 1st, 15th and 27th for the period from April, 1th till June, 30th. Fig. 6 shows daily forecast ensembles for this period compared to the observed inflow data.



1
2 **Figure 6: The ESP-based forecast of daily inflow discharge for the period from April, 1th till June, 30th issued on March 1st (a)**
3 **and March 27th (b). Thin blue lines – ensemble of the forecasted hydrographs; bold blue line – mean ensemble hydrograph, red**
4 **line – observed hydrograph of inflow into the Cheboksary reservoir.**

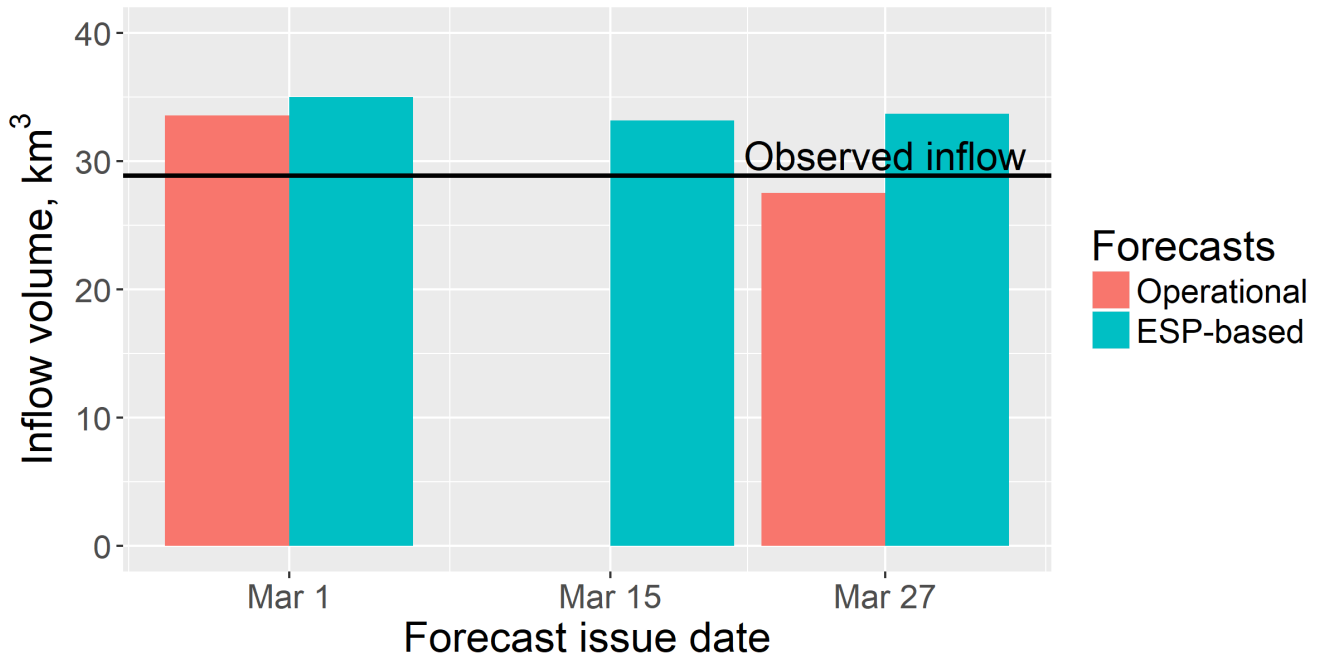
5 Box plots of the ESP-based forecasts of different inflow characteristics are presented in Fig 7. All forecasts of inflow volume
6 showed low errors (Fig. 7a), unlike the maximum discharge forecasts (Fig. 7b), however, the Q_{\max} forecast range envelopes
7 the observed maximum inflow discharge. Both forecasts of number of days over thresholds showed low errors (Fig. 7b, d),
8 e.g. just before the beginning of April we correctly forecasted low freshet with the absence of days when inflow discharge
9 exceeds the mean maximum discharge for the period of observations.

10 In 2017, Roshydromet also issued forecast of spring water inflow into the Cheboksary reservoir on the basis of the
11 methodology presented above (Fig. 8). In contrast with the results presented in Table 1 and Fig. 4, which demonstrate
12 general advantage of the ESP-based forecasts over the operational forecasts for 1982-2016, in 2017, operational forecast of
13 inflow volume appeared to be more preferable. Possible explanation is again in errors in simulated pre-melt SWE used as
14 initial conditions for the ESP-based forecast.



1

2 **Figure 7: Box plots of the ESP-based forecast of inflow volume (a), maximum inflow discharge (c), number of days with inflow**
 3 **discharge above mean observed discharge (b), and number of days with inflow discharge above mean maximum observed**
 4 **discharge (d) for the period from April, 1th till June, 30th of 2017**



1

2 **Figure 8: The ESP-based and operational forecasts of volume of water inflow into the Cheboksary reservoir for the period of**
 3 **01/04/2017-30/06/2017 (line presents the observed value)**

4 **4.3.3 Probabilistic forecast**

5 In this section, the operational forecast, which is issued in deterministic form only, is not discussed.

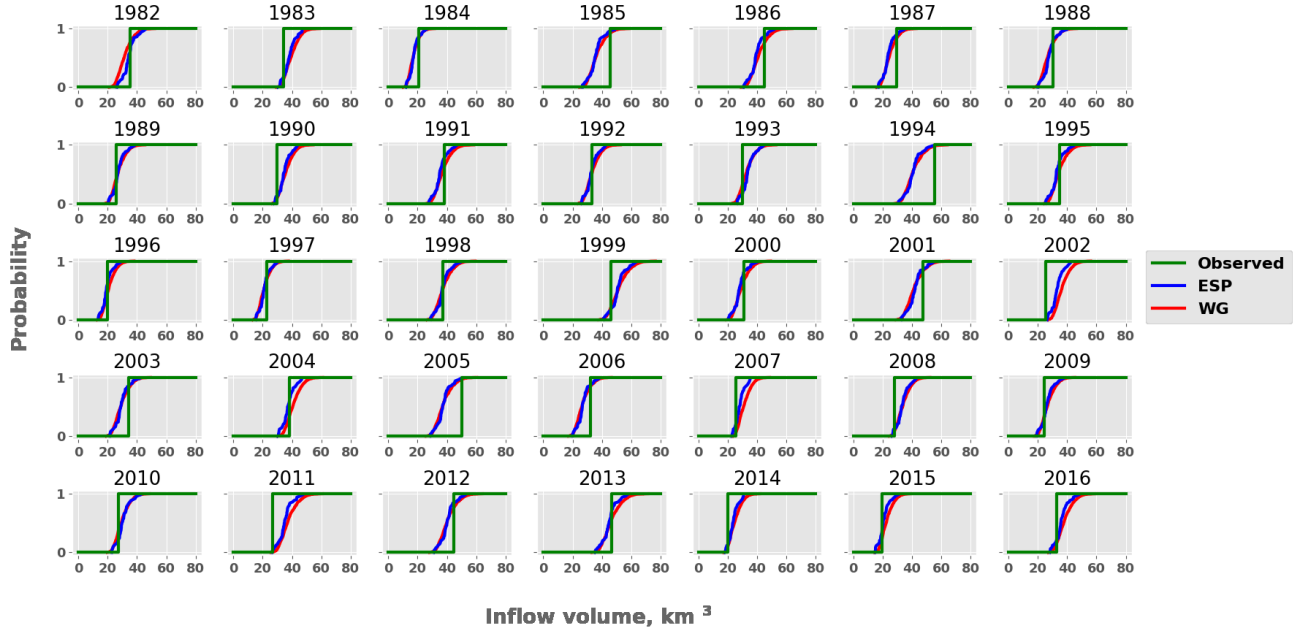
6 One of the main advantage of the ensemble forecasting is the ability to assess the uncertainty that is nested in the future
 7 possible behavior of the hydrological system. The resulting ensemble is used to create cumulative distribution function
 8 (CDFs) of the desired characteristic in j^{th} forecast as

9
$$F_m(j) = \sum_{i=1}^m f_i(j), m=1, \dots, M; j=1, \dots, N, \quad (4)$$

10 where M are the forecast probability bins on the interval $[0;1]$; N – total number of forecasts; f_i – probability of forecast in
 11 m^{th} bin.

12 CDFs of the forecasted inflow volume W for the period from April, 1 to June, 30 of 35 years (1982-2016) are shown in
 13 Fig. 9. Three CDFs are combined in each plot: two CDFs of forecasts calculated under ESP-based and WG-based weather
 14 scenarios, and CDF of the observed inflow volume in the specific year (CDFs of observations can be represented as the
 15 Heaviside step function). One can see from Fig. 9 that for the most of the years the inflow is not far from the most probable
 16 one, in other words, CDF of the forecasts crosses CDF of observations around 50% probability. For almost all years

1 observed inflow lies within the range of the ensemble. Exceptions are 1994, 2002, 2005 and 2011, i.e. once per 8-9 years, on
 2 average, ensemble forecast range does not cover observed inflow because of large forecast errors.



3
 4 **Figure 9: Cumulative probability distribution functions for W in April – June for all years between 1982 and 2016. Green line –**
 5 **observed inflow, orange – ESP-based forecast, blue – WG-based forecast**

6
 7 To quantify an ability of forecasts to predict probability of the event occurred within the pre-assigned inflow categories, we
 8 used the RPS measure. The forecast efficiency was measured by the RPSS criterion relating the verified forecast to
 9 streamflow climatology (both RPS and RPSS formulations are presented in Table 1S)

10 Both forecasts demonstrate moderate improvement over climatology: according to the RPSS value, around 30% on average
 11 both for W and for Q_{max} (Table 3). Probably, accounting for a seasonal weather forecast and conditioning historical weather
 12 patterns on this forecast could result in a higher improvement over the streamflow climatology, however a reliable seasonal
 13 weather forecast for the study region is not available.

14 In addition, we compared the ESP-based and the WG-based forecasts by setting the former one as a reference forecast. The
 15 modified RPSS is formulated in this case as:

16
$$RPSS_{\text{modified}} = 1 - \frac{RPS_{WG}}{RPS_{ESP}} \quad (5)$$

1 **Table 3. Ranked Probability Score and Skill score for the forecasts**

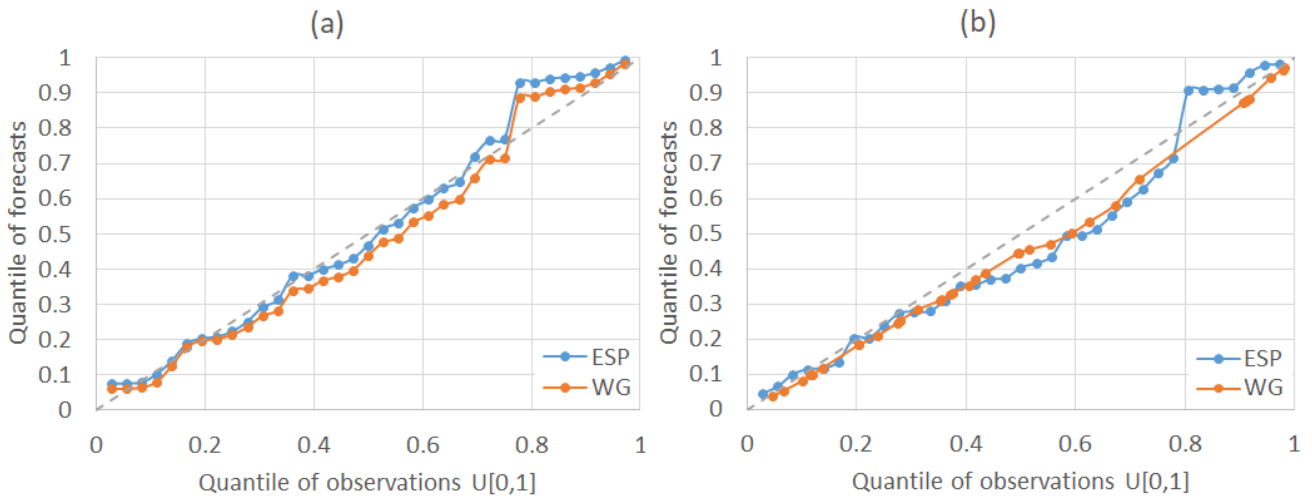
Inflow characteristics	RPS_{ESP}	RPSS (ESP vs. climatology)	RPS_{WG}	RPSS (WG vs. climatology)	RPSS _{modified} (WG vs. ESP)
W	0.33	0.38	0.38	0.28	-0.16
Q_{max}	0.43	0.28	0.49	0.20	-0.13

2 As one might expect from a comparison of the unmodified RPSS measures, the modified one showed that the WG forecasts
 3 are less skillful than the ESP with modified RPSS values of -0.16 for W and -0.13 for Q_{max} .

4 To compare quantiles of the forecasted characteristics with the quantiles of the corresponding observations, we used the
 5 predictive Q-Q plot (Laio and Tamea, 2007). As one can see from Fig. 10a, the predictive Q-Q plot of the inflow volume
 6 forecasts demonstrates good agreement with the distribution of the observations. This is fairly consistent for both
 7 methodologies and for all quantiles, but for rare events there is an underestimation of the predictive uncertainty, expressed as
 8 an offset of 1:1 line in the upper right corner of the plot. For the maximum inflow discharge (Fig. 10b), one can see
 9 overprediction in both methodologies. However, the behavior of ESP-based and WG-based forecasts of rare events is
 10 different in terms of predictive uncertainty. Particularly, the WG-based forecasts of the events of low exceedance probability
 11 appeared to be closer to the 1:1 line.

12 Additional comparative features of the ensemble forecasts of both types, one can detect from the reliability and
 13 discrimination diagrams presented in Figs. 9S-12S of the Supplementary Materials.

14 Overall, all presented measures of the probabilistic forecast performance are slightly better for the ESP-based forecasts than
 15 for the WG-based forecasts, though the differences are not significant and hardly interpretable. At the same time, verification
 16 measures obtained from the large ensemble of the WG-based forecasts should be more statistically reliable, that is
 17 demonstrated in the next section for two measures: CDF and RPSS.



1 **Figure 10: Predictive quantile-quantile plots for inflow volume (a) and inflow discharge (b) forecasts**

2 **4.3.4 Ensemble size effect on the verification measures: two examples**

3 It can be seen from Fig. 9 that the CDFs appeared to be close to each other for both used ensemble methodology. However,
4 the sample variance of the CDF is significantly different due to different amount of scenarios in the ensembles: 51 in the
5 ESP-based ensemble and 1000 in the WG-based ensemble. To illustrate such difference, we assessed confidence bands for
6 CDFs derived from both forecasting approaches. A two sided confidence bands were expressed from Dvoretzky-Kiefer-
7 Wolfowitz inequality as (e.g. Massart, 1990):

$$8 \quad \mathbb{P}\left(\sup_{x \in \mathcal{R}} |\hat{F}_n(x) - F(x)| \geq \varepsilon\right) \leq 2 \exp(-2n\varepsilon^2) \quad (6)$$

9 where $F(x)$ and $\hat{F}_n(x)$ are the CDF's ordinate and its empirical estimation from a sample of size n , respectively; ε is the
10 constant depending on the significance level α as

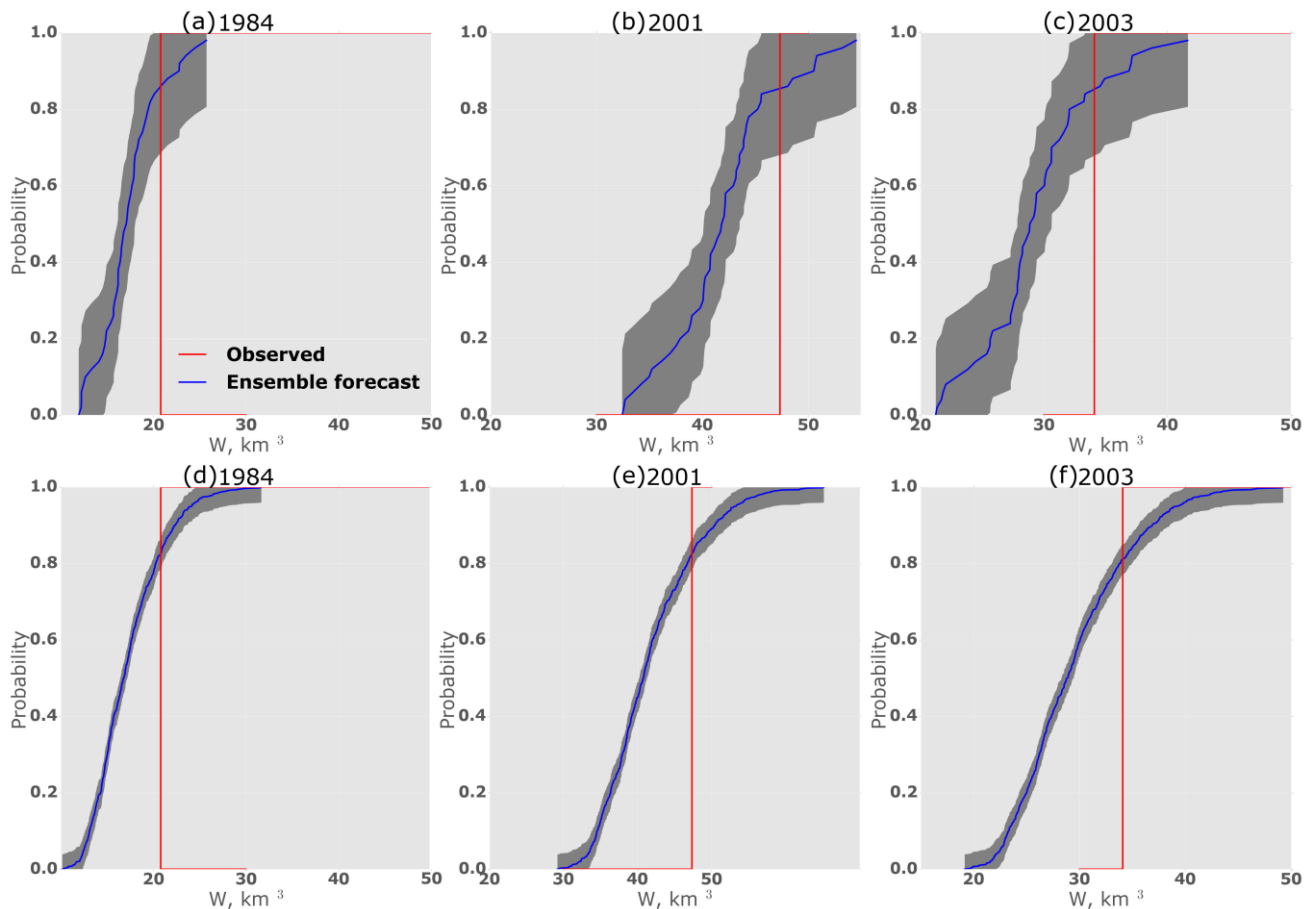
$$11 \quad \varepsilon = \sqrt{\frac{1}{2n} \ln\left(\frac{2}{1-\alpha}\right)} \quad (7).$$

12 For the pre-assigned confidence probability $p=(1-\alpha)$, the upper ($U(x)$) and the lower ($L(x)$) confidence bands of the empirical
13 CDF $\hat{F}_n(x)$ are defined from (5) and (6) as:

$$14 \quad U(x) = \min[\hat{F}_n(x) + \varepsilon, 1] \quad (8)$$

$$15 \quad L(x) = \max[\hat{F}_n(x) - \varepsilon, 0] \quad (9)$$

16 Fig. 11 demonstrates difference between 95%-confidence intervals of the ESP-based inflow volume forecast as compared to
17 the corresponding intervals of the WG-based forecast. We believe that this difference should be taken into account by the
18 ensemble forecast developers when they use statistical verification measures for assessment of forecast performance, as well
19 as by the users when they interpret the forecast.



1
2 **Figure 11: Cumulative probability distribution functions for W in April – June for selected years between 1982 and 2016 for ESP-**
3 **based forecast (a – c) and WG-based forecast (d – f). Shaded area presents confidence interval of 95% confidence probability.**

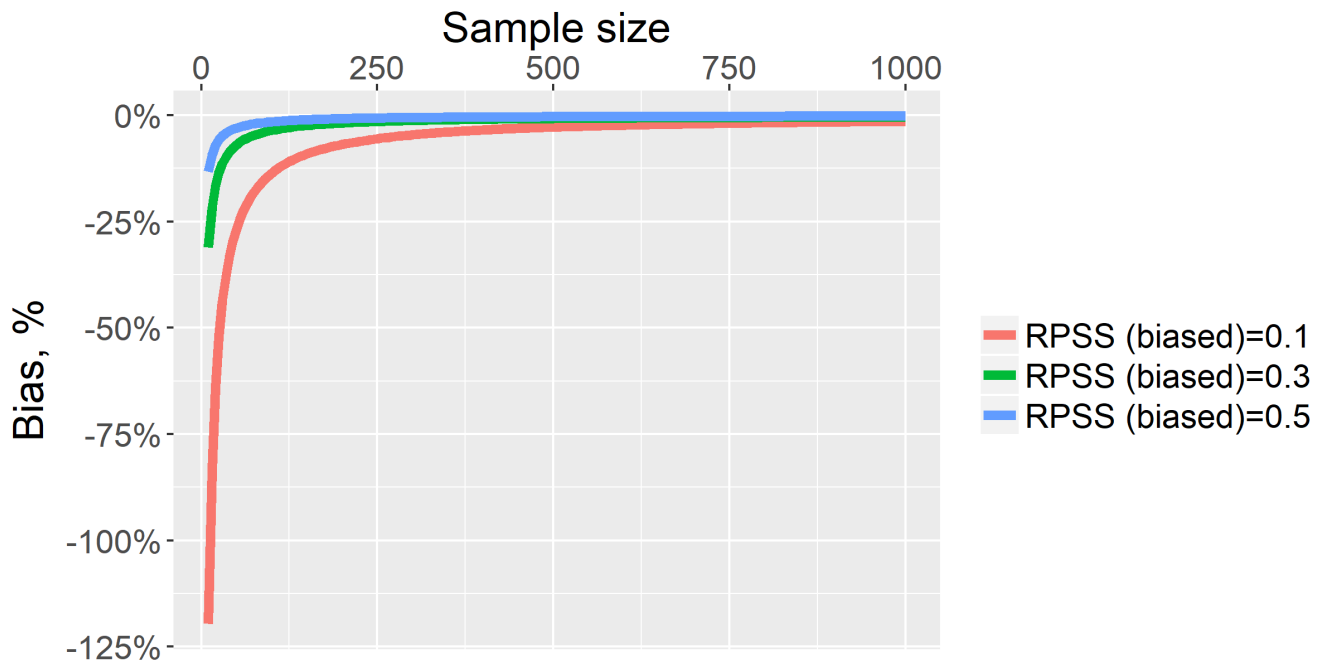
4 One can conclude from Table 3 that RPSS criterion demonstrates advantage of the ESP-based probabilistic forecast over the
5 WG-based one as compared to climatology. However, it is important to take into account that the RPSS measure is strongly
6 dependent on ensemble size and negatively biased (see, for instance, Müller et al. 2005, Weigel et al., 2007). A debiased
7 estimate of RPSS can be formulated as (Weigel et al., 2007):

8

$$RPSS_D = 1 - \frac{RPS}{RPS_{ref} + D} \quad (10)$$

9 where D is the correction term depending on the ensemble size, the climatological probabilities, and the number of
10 categories. For very large ensemble size, the correction term D converges toward zero and the $RPSS_D$ toward the RPSS.

11 Fig. 12 demonstrates the dependence of the RPSS bias on sample size built with the use of approximation of D presented in
12 (Weigel et al., 2007).



1

2 **Figure 12: Negative bias of the RPSS-estimate in dependence on the ensemble size and the RPSS value**

3 One can see from this Fig. 12 that under the used 51-member ensemble (i.e. the ESP-based ensemble) the bias can reach tens
 4 of percent depending on the RPSS estimate. Under the used 1000-member ensemble, the bias is close to zero.

5 **5 Conclusions**

6 The paper describes the development and preliminary assessment results of the long-term forecasting methodology for the
 7 water inflow into the Cheboksary reservoir – one of the eleven major river reservoirs of the Volga-Kama Reservoir Cascade.
 8 The methodology is based on a combination of semi-distributed hydrological model ECOMAG that allows for ensemble
 9 calculation of inflow hydrographs with the two different sets of weather ensembles for the lead-time period: observed
 10 weather data constructed on the basis of the ESP methodology, and synthetic weather data simulated by a weather generator.
 11 As it is mentioned in the Introduction section, we studied: (1) whether there is any advantage of the developed ensemble
 12 forecasts in comparison with the currently issued operational forecasts of water inflow into the Cheboksary reservoir, and (2)
 13 whether there is any noticeable improvement in the probabilistic forecasts when using the WG-simulated ensemble
 14 compared to the ESP-based ensemble.

15 Our findings can be summarised as follows:

- 16 1. For the 35-year period starting from the reservoir filling in 1982, both continuous and binary model-based ensemble
 17 forecasts (issued in deterministic form), overperformed the operational forecasts (currently used in practice) of the

1 April-June inflow volume. However, for several years (including 2017), the operational forecasts were more
2 accurate in terms of the absolute errors. We found that the larger errors of the ensemble forecasts in these years
3 were resulting from the errors in the modelled initial snow water equivalent on the forecast issue date comparing
4 with the observed SWE. The prospects for improving the ensemble forecasts are in assimilation of the observation
5 data (accounting for their reliability) on the forecast issue date.

- 6 2. Model-based ensemble approach extended a list of the forecasted inflow characteristics in comparison with the
7 operational forecast. In addition to the inflow volume for the period of April-June, both ESP-based and WG-based
8 methodology provided acceptable forecasts of maximum inflow discharge, number of days with inflow discharge
9 above the mean observed discharge, and number of days with inflow discharge above the mean maximum observed
10 discharge for this period. Thus, the ensemble methodology enhanced the informational content of the forecast in
11 comparison with the operational one.
- 12 3. Overall, all the presented measures of the deterministic and probabilistic forecast performance are slightly better for
13 the ESP-based forecasts than for the WG-based forecasts, though the differences are not significant and hardly
14 interpretable. At the same time, verification measures obtained from the large ensemble of the WG-based forecasts
15 appear to be more statistically reliable than the measures obtained from the ensemble size limited to the number of
16 the historical years.

17 Currently we are in the process of updating and fine-tuning the presented forecast methodology for its practical tests during
18 the freshet of 2018.

19 Our further research will be aimed at the following:

- 20 1. Refinement of the initial (on the forecast issue date) basin conditions through assimilation of the available
21 observation data, first of all snow observations, into the hydrological model. Ensemble Kalman filtering is seen as
22 as a promising procedure for that.
- 23 2. Use of the medium-range and seasonal weather forecasts for pre-processing the weather scenarios (both the ESP-
24 based and the WG-based) for the hydrological forecast lead-time time.

26 **Acknowledgements**

27 The authors are very grateful to three anonymous Reviewers for criticisms and constructive comments. Also, we would like
28 to thank to Ilias Pechlivanidis (handling editor) for his valuable suggestions.

29 The research related to developing methods of ensemble forecast and forecast verification technique was financially
30 supported by the Russian Foundation for Basic Research (grants No. 16-05-00679 and 16-05-00599). The other research
31 components, including those related to comparison of the ensemble forecast with the operational one, were financially
32 supported by the Russian Science Foundation (grant No. 17-77-30006).

1 The present work was carried out within the framework of the Panta Rhei Research Initiative of the International Association
2 of Hydrological Sciences (IAHS).

3 **References**

- 4 Abrahart, R. J., Anctil, F., Coulibaly, P., Dawson, C. W., Mount, N. J., See, L. M., Shamseldin, A. Y., Solomatine, D. P.,
5 Toth, E. and Wilby, R. L.: Two decades of anarchy? Emerging themes and outstanding challenges for neural network
6 river forecasting, *Prog. Phys. Geogr.*, doi:10.1177/0309133312444943, 2012.
- 7 Arnal, L., Wood, A. W., Stephens, E., Cloke, H. L. and Pappenberger, F.: An Efficient Approach for Estimating Streamflow
8 Forecast Skill Elasticity, *J. Hydrometeorol.*, doi:10.1175/JHM-D-16-0259.1, 2017.
- 9 Avakyan A.B.: Volga-Kama cascade reservoirs and their optimal use. *Lakes and Reservoirs Research and Management*,
10 3:113 – 121, 1998
- 11 Beckers, J. V. L., Weerts, A. H., Tijdeman, E. and Welles, E.: ENSO-conditioned weather resampling method for seasonal
12 ensemble streamflow prediction, *Hydrol. Earth Syst. Sci.*, doi:10.5194/hess-20-3277-2016, 2016.
- 13 Borsch, S. and Simonov, Y.: Operational Hydrologic Forecast System in Russia, in *Flood Forecasting: A Global*
14 *Perspective.*, 2016.
- 15 Buizza, R. and Palmer, T. N.: Impact of Ensemble Size on Ensemble Prediction, *Mon. Weather Rev.*, doi:10.1175/1520-
16 0493(1998)126<2503:IOESOE>2.0.CO;2, 1998.
- 17 Caraway, N. M., McCreight, J. L. and Rajagopalan, B.: Multisite stochastic weather generation using cluster analysis and k-
18 nearest neighbor time series resampling, *J. Hydrol.*, doi:10.1016/j.jhydrol.2013.10.054, 2014.
- 19 Chemerenko, E.P.: Long-term forecasting of spring inflow into the Cheboksary reservoir. *Proceedings of the*
20 *Hydrometeorological centre of Russia (in Russian)*. Vol. 324. P. 16-21, 1992
- 21 Day, G. N.: Extended Streamflow Forecasting Using NWSRFS, *J. Water Resour. Plan. Manag.*, doi:10.1061/(ASCE)0733-
22 9496(1985)111:2(157), 1985.
- 23 Demirel, M. C., Booij, M. J. and Hoekstra, A. Y.: The skill of seasonal ensemble low-flow forecasts in the Moselle River for
24 three different hydrological models, *Hydrol. Earth Syst. Sci.*, doi:10.5194/hess-19-275-2015, 2015.
- 25 Druce, D. J.: Insights from a history of seasonal inflow forecasting with a conceptual hydrologic model, *J. Hydrol.*,
26 doi:10.1016/S0022-1694(01)00415-2, 2001.
- 27 Ferro, C. A. T. and Stephenson, D. B.: Extremal Dependence Indices: Improved Verification Measures for Deterministic
28 Forecasts of Rare Binary Events, *Weather Forecast.*, doi:10.1175/WAF-D-10-05030.1, 2011.

- 1 Franz, K. J. and Hogue, T. S.: Evaluating uncertainty estimates in hydrologic models: Borrowing measures from the forecast
2 verification community, *Hydrol. Earth Syst. Sci.*, doi:10.5194/hess-15-3367-2011, 2011.
- 3 Gelfan, A. N. and Motovilov, Y. G.: Long-term hydrological forecasting in cold regions: Retrospect, current status and
4 prospect, *Geogr. Compass*, doi:10.1111/j.1749-8198.2009.00256.x, 2009.
- 5 Gelfan, A. N., Motovilov, Y. G. and Moreido, V. M.: Ensemble seasonal forecast of extreme water inflow into a large
6 reservoir, in *IAHS-AISH Proceedings and Reports.*, 2015.
- 7 Gelfan, A., Gustafsson, D., Motovilov, Y., Arheimer, B., Kalugin, A., Krylenko, I. and Lavrenov, A.: Climate change impact
8 on the water regime of two great Arctic rivers: modeling and uncertainty issues, *Clim. Change*, doi:10.1007/s10584-
9 016-1710-5, 2017.
- 10 Gelfan, A.: Extreme snowmelt floods: Frequency assessment and analysis of genesis on the basis of the dynamic-stochastic
11 approach, *J. Hydrol.*, doi:10.1016/j.jhydrol.2010.04.031, 2010.
- 12 Gottschalk, L., Beldring, S., Engeland, K., Tallaksen, L., Sælthun, N. R., Kolberg, S. and Motovilov, Y.:
13 Regional/macroscale hydrological modelling: a Scandinavian experience, *Hydrol. Sci. J.*,
14 doi:10.1080/02626660109492889, 2001.
- 15 Hanes, W. T., Fogel, M. M. and Duckstein, L.: Forecasting Snowmelt Runoff: Probabilistic Model, *J. Irrig. Drain. Div.*,
16 1977.
- 17 Hartmann, H. C., Pagano, T. C., Sorooshian, S. and Bales, R.: Confidence builders: Evaluating seasonal climate forecasts
18 from user perspectives, *Bull. Am. Meteorol. Soc.*, doi:10.1175/1520-0477(2002)083<0683:CBESCF>2.3.CO;2, 2002.
- 19 Kuchment, L. S. and Gelfan, A. N.: Long-term probabilistic forecasting of snowmelt flood characteristics and the forecast
20 uncertainty. In: Boegh, E., Kunstmann, H., Wagener, T., Hall, A., Bastidas, L., Franks, S., Gupta, H., Rosbjerg, D.,
21 and Schaake, J. (eds) Quantification and reduction of predictive uncertainty for sustainable water resources
22 management, Vol. 313. Wallingford, UK: IAHS Publishers, p. 213–221, 2007
- 23 Laio, F. and Tamea, S.: Verification tools for probabilistic forecasts of continuous hydrological variables, *Hydrol. Earth
24 Syst. Sci. Discuss.*, doi:10.5194/hessd-3-2145-2006, 2006.
- 25 Lettenmaier, D.P. and Waddle, T.J.: Forecasting Seasonal Snowmelt Runoff: A Sum-mary of Experience with Two Models
26 Applied to Three Cascade Mountain, Washington Drainages, *WRS 59. – 1978. – 97 P.*, 1978
- 27 Li, H., Luo, L., Wood, E. F. and Schaake, J.: The role of initial conditions and forcing uncertainties in seasonal hydrologic
28 forecasting, *J. Geophys. Res. Atmos.*, doi:10.1029/2008JD010969, 2009.
- 29 Massart, P.: The Tight Constant in the Dvoretzky-Kiefer-Wolfowitz Inequality, *Ann. Probab.*, doi:10.1214/aop/1176990746,
30 1990.

- 1 McEnery, J., Ingram, J., Duan, Q., Adams, T. and Anderson, L.: NOAA's advanced hydrologic prediction service: Building
2 pathways for better science in water forecasting, *Bull. Am. Meteorol. Soc.*, doi:10.1175/BAMS-86-3-375, 2005.
- 3 McKay, M. D., Beckman, R. J. and Conover, W. J.: A comparison of three methods for selecting values of input variables in
4 the analysis of output from a computer code, *Technometrics*, doi:10.1080/00401706.2000.10485979, 2000.
- 5 Mendoza, P. A., Wood, A. W., Clark, E., Rothwell, E., Clark, M. P., Nijssen, B., Brekke, L. D. and Arnold, J. R.: An
6 intercomparison of approaches for improving operational seasonal streamflow forecasts, *Hydrol. Earth Syst. Sci.*,
7 doi:10.5194/hess-21-3915-2017, 2017.
- 8 Motovilov, Y. G.: Hydrological simulation of river basins at different spatial scales: 1. Generalization and averaging
9 algorithms, *Water Resour.*, 43(3), 429–437, doi:10.1134/S0097807816030118, 2016.
- 10 Motovilov, Yu., Gottschalk, L., Engeland, K., and Belokurov, A.: ECOMAG – regional model of hydrological cycle.
11 Application to the NOPEX region. Department of Geophysics, University of Oslo, Institute Report Series no. 105, 88
12 p., 1999.
- 13 Müller, W. A., Appenzeller, C., Doblas-Reyes, F. J. and Liniger, M. A.: A debiased ranked probability skill score to evaluate
14 probabilistic ensemble forecasts with small ensemble sizes, *J. Clim.*, doi:10.1175/JCLI3361.1, 2005.
- 15 Najafi, M. R. and Moradkhani, H.: Ensemble Combination of Seasonal Streamflow Forecasts, *J. Hydrol. Eng.*,
16 doi:10.1061/(ASCE)HE.1943-5584.0001250, 2016.
- 17 Najafi, M. R., Moradkhani, H. and Piechota, T. C.: Ensemble Streamflow Prediction: Climate signal weighting methods vs.
18 Climate Forecast System Reanalysis, *J. Hydrol.*, doi:10.1016/j.jhydrol.2012.04.003, 2012.
- 19 Nash, J. E. and Sutcliffe, J. V.: River flow forecasting through conceptual models part I - A discussion of principles, *J.*
20 *Hydrol.*, doi:10.1016/0022-1694(70)90255-6, 1970.
- 21 Pappenberger, F. et al.: Hydrological Ensemble Prediction Systems Around the Globe, in *Handbook of Hydrometeorological*
22 *Ensemble Forecasting*, edited by Q. Duan, F. Pappenberger, J. Thielen, A. Wood, H. L. Cloke, and J. C. Schaake, pp.
23 1–35, Springer Berlin Heidelberg, Berlin, Heidelberg., 2016.
- 24 Press, W. H., Teukolsky, S. A., Vetterling, W. T. and Flannery, B. P.: *Numerical Recipes 3rd Edition: The Art of Scientific*
25 *Computing.*, 2007.
- 26 Richardson, D. S.: Measures of skill and value of ensemble prediction systems, their interrelationship and the effect of
27 ensemble size, *Q. J. R. Meteorol. Soc.*, doi:10.1256/smsqj.57714, 2001.
- 28 Shukla, S. and Lettenmaier, D. P.: Seasonal hydrologic prediction in the United States: Understanding the role of initial
29 hydrologic conditions and seasonal climate forecast skill, *Hydrol. Earth Syst. Sci.*, doi:10.5194/hess-15-3529-2011,
30 2011.

- 1 Svanidze, G. G.: Mathematical Modeling of Hydrologic Series. Water Resources Publications, Fort Collins, Colorado, USA,
2 324 p., 1980
- 3 Taylor, K. E.: Summarizing multiple aspects of model performance in a single diagram, *J. Geophys. Res. Atmos.*,
4 doi:10.1029/2000JD900719, 2001.
- 5 Weigel, A. P., Liniger, M. A. and Appenzeller, C.: Generalization of the Discrete Brier and Ranked Probability Skill Scores
6 for Weighted Multimodel Ensemble Forecasts, *Mon. Weather Rev.*, doi:10.1175/MWR3428.1, 2007.
- 7 Wilks, D. S.: Statistical methods in the atmospheric sciences, *Int. Geophys. Ser.*, doi:10.1007/s13398-014-0173-7.2, 1995.
- 8 Wood, A. W. and Lettenmaier, D. P.: A test bed for new seasonal hydrologic forecasting approaches in the western United
9 States, *Bull. Am. Meteorol. Soc.*, doi:10.1175/BAMS-87-12-1699, 2006.
- 10 Yossef, N. C., Winsemius, H., Weerts, A., Van Beek, R. and Bierkens, M. F. P.: Skill of a global seasonal streamflow
11 forecasting system, relative roles of initial conditions and meteorological forcing, *Water Resour. Res.*,
12 doi:10.1002/wrcr.20350, 2013.
- 13 Zmieva E.S.: Forecasts of water inflow into the Kuibyshevskoe and Volgogradskoe reservoirs (in Russian). Gidrometizdat.
14 Moscow., 255 p., 1964
15